Biochemical and Biophysical Research Communications 421 (2012) 514–520

Contents lists available at SciVerse ScienceDirect

Biochemical and Biophysical Research Communications

journal homepage: www.elsevier.com/locate/ybbrc

Structural and enzymatic properties of an *in vivo* proteolytic form of PD-S2, type 1 ribosome-inactivating protein from seeds of *Phytolacca dioica* L.

Antimo Di Maro [a,*], Rita Berisio [b], Alessia Ruggiero [b], Rachele Tamburino [a], Valeria Severino [a], Enza Zacchia [a], Augusto Parente [a]

[a] Dipartimento di Scienze della Vita, Seconda Università di Napoli, Via Vivaldi 43, I-81100 Caserta, Italy
[b] Istituto di Biostrutture e Bioimmagini, C.N.R., Via Mezzocannone 16, I-80134 Napoli, Italy

ARTICLE INFO

Article history:
Received 2 April 2012
Available online 10 April 2012

Keywords:
3D modeling
Circular dichroic spectroscopy
Proteolytic regulation
Phytolacca dioica
Ribosome-inactivating proteins

ABSTRACT

PD-S2, type 1 ribosome-inactivating protein from *Phytolacca dioica* L. seeds, is an *N*-β-glycosidase likely involved in plant defence. In this work, we purified and characterized an *in vivo* proteolytic form of PD-S2, named cutPD-S2. Spectroscopic characterization of cutPD-S2 showed that the proteolytic cleavage between Asn195 and Arg196 does not alter the protein fold, but significantly affects its thermal stability. Most importantly, the proteolytic cleavage induces a 370-fold decrease of PD-S2 capacity of inhibiting *in vitro* protein biosynthesis.

Our data catch the turning point from a typical role of PD-S2 as a defence protein to that of supplier of essential amino acids during seedling development.

1. Introduction

Ribosome-inactivating proteins (RIPs) are *N*-glycosidases (EC 3.2.2.22) widely distributed in nature but predominantly found in plants, fungi and bacteria [1]. They remove a specific adenine (A 4324 of the 28S rRNA in rat ribosomes) from the sarcin/ricin loop of the large rRNA, thus arresting protein synthesis at the translocation step [2]. RIPs are also able to remove adenine from various polynucleotides other than RNA and are more generally considered as adenine polynucleotide glycosylases (APG) [3]. RIPs display antiviral, antibacterial and antifungal activities [4] and, as such, they possess potential applications in medicine and in agriculture [5]. For example, expression or administration of type 1 RIPs could limit virus or fungal pathogens replication [4,6], while type 2 RIPs may inhibit the proliferation of cancer cells [7]. They are classified as types 1, 2, or 3 according to their structure [2].

Phytolacca dioica L. produces a suite of type 1 RIPs in its seeds and leaves [8]. The expression in leaves presents a seasonal and age regulation. For instance PD-Ls 1–4, 30 kDa RIPs, are found in *P. dioica* fully expanded leaves [9–11], but not in leaves of young *P. dioica* (8–36 month old), where they are replaced by two novel type 1 RIPs, dioicin 1 and dioicin 2 [12]. In developing leaves of adult plants (10–60 days old), PD-Ls 1–4 and dioicin 2 are always present, whereas dioicin 1 can be detected only in restricted growth times (10–17 days old) [12].

Three *N*-glycosylated RIPs (PD-S 1–3) are found in seeds of *P. dioica*; they differ for their sugar content. Among these 30 kDa constitutive RIPs, PD-S2, the major form (86 mg/100 g seeds [13]), was well characterized in our laboratory [13,14]. While studying PD-S2, it came to our attention that the chromatographic peak of the last purification step of PD-S2 contained also a minor form, which could be detected only on the SDS–PAGE in reducing conditions. Here, we show that this minor form is a proteolyzed version of PD-S2, hereafter named cutPD-S2. We report the purification to homogeneity of cutPD-S2, its thorough biochemical and enzymatic characterization coupled with molecular modeling identifying the likely structural determinants of the enzyme altered activity. These results, together with the analysis of the fate of PD-S2 during seedling, identify the very first step of PD-S2 proteolysis, observed also in other plants [15], which eventually delivers essential amino acids as possible source of building blocks for plant development [16,17].

2. Materials and methods

2.1. Purification of cutPD-S2 from seeds of P. dioica

Purification of cutPD-S2 from PD-S2 was performed by RP-HPLC on a C-4 semipreparative column [250 × 10 mm, 5 μm particle size

Abbreviations: 2-Me, 2-β-mercaptoethanol; DTT, dithiothreitol; Gdn · Cl, guanidinium chloride; hsDNA, herring sperm DNA; PD-S2, major form of ribosome-inactivating proteins from seeds of *P. dioica*.

* Corresponding author. Fax: +39 0823 274535.
E-mail address: antimo.dimaro@unina2.it (A. Di Maro).

0006-291X/$ - see front matter © 2012 Elsevier Inc. All rights reserved.
http://dx.doi.org/10.1016/j.bbrc.2012.04.036

(Phenomenex, Torrance, CA-USA)], mounted on a Breeze® instrument (Waters Italia SpA, Milano, Italy). In detail, the ascending part of the PD-S2 peak from the CM-Sepharose chromatography (see the Supplemental material for the PD-S2 purification), was loaded on the semipreparative column, which was eluted with a discontinuous gradient of solvent A and B (Table S1), at a flow rate of 2.5 mL/min, where A and B were 0.1% TFA in MilliQ water and acetonitrile containing 0.1% TFA, respectively. To remove TFA and acetonitrile, pure cutPD-S2 was dialysed against 6 M Gdn · Cl in 10 mM Tris · Cl, pH 8.4, and renatured through extensive dialysis against the same buffer and decreasing Gdn · Cl concentrations (from 6 to 0.0 M). The protein solution was concentrated, aliquoted, and then stored at −20 °C. The same procedure was applied to the control PD-S2 purified by RP-HPLC, hereafter named hplcPD-S2. Homogeneity of purified proteins was determined by SDS–PAGE, with and without 2-mercaptoethanol, on a Mini-Protean II mini-gel apparatus (Bio-Rad; Milano, Italy), using 6% (w/v) stacking polyacrylamide gel and 12% (w/v) separation gel [18].

2.2. Selective reduction of disulfide bridges with DTT

For selective reduction of disulfide bridges, to cutPD-S2 samples (~15 μg, 0.5 nmol), dissolved in 10 mM Tris · Cl, pH 8.4, suitable volumes of 8 M Gdn · Cl were added to obtain a concentration of 1.0, 2.0, 3.0, 4.0, 5.0 and 6.0 M; a sample without Gdn · Cl was also analyzed. Then, DTT (5× molar excess on the protein) was added to the samples in a final volume of 100 μL, incubating for 30 min, at 25 °C. Alkylation was obtained adding iodoacetamide (0.4 M IAM) to the protein solution at 1:4 ratio (DTT:IAM; mol:mol), with 5 min incubation time. Samples were then directly analyzed by RP-HPLC on a Vydac C4 column (0.46 × 25 cm; 5 μm particle size), eluted with a linear gradient from 5% to 65% of solvent B over 60 min, at a flow rate of 1 mL/min. Eluted proteins or peptides were monitored at 214 nm. To verify the carboxymethyl cysteine amount, similar experiments were also carried out using 4 M Gdn · Cl, at two different concentrations of DTT (5 and 10× on the protein), incubating for 30 min, at 25 °C. Then, the samples were subjected to acid hydrolysis for amino acid analyses (see Supplementary material).

2.3. Circular dichroism spectroscopy

CD spectra were recorded at room temperature using a Jasco J-810 spectropolarimeter equipped with a Peltier thermostatic cell holder [19]. Molar ellipticity per mean residue, $[\Theta]$ in deg cm^2 dmol^{-1}, was calculated from the equation: $[\Theta] = [\Theta]\text{obs mw}/10\,l\,C$, where $[\Theta]$obs is the ellipticity measured in milli-degrees, mw is the mean residue molecular weight, C is the protein concentration in g L^{-1} and l is the optical path length of the cell in cm. Far-UV measurements (260–190 nm) were carried out using a 0.1 cm path length cell and protein concentration 0.3 mg/mL in 20 mM Na · acetate, pH 4.6. CD spectra were signal averaged over at least three scans and the baseline corrected by subtracting the buffer spectrum. Thermal unfolding curves were recorded in the temperature mode at 222 nm.

2.4. Functional assays

Inhibition of protein synthesis by PD-S2 and cutPD-S2 in a lysate of rabbit reticulocytes was performed as previously described [20]. Results are mean values of three experiments performed in duplicate. Polynucleotide–adenosine glycosidase activity was assayed on both herring sperm DNA (hsDNA) and poly(A) (Sigma–Aldrich, Milano, Italy) [21]. The amount of released bases in the supernatant was measured spectrophotometrically at 260 nm. Results were reported as percentage of native PD-S2 activity.

2.5. Homology modeling studies

The three-dimensional structure of PD-S2 was modeled by comparative protein modeling methods using the SWISS-MODEL workspace [22]. The model was built using the 2.2 Å resolution structure of pokeweed antiviral protein (Protein Data Bank entry 1APA), as a template. The degree of sequence identity between the template and PD-S2 is 78%, which enabled us to generate a reliable model. This model was energetically minimized using GROMACS [23].

3. Results

3.1. P. dioica seeds contain two different forms of PD-S2

SDS–PAGE analysis of purified PD-S2 from the CM-Sepharose column, performed in non-reducing conditions produced a single band (thus suggesting the presence of a single form of PD-S2) [8,13]. However, when we analyzed the single fractions of the eluted peak (from the CM-Sepharose chromatography) in reducing conditions (region 'a' of the chromatogram in Fig. S1) we observed in the ascending part of the peak the presence of the 30 kDa form (~75%) and two additional bands (~25%) with lower molecular weights (24 and 6.5 kDa; insert in Fig. 1S). We then decided to sequence these bands, transferred onto PVDF membranes, by Edman degradation. This analysis unequivocally showed that the band at 24 kDa was a shorter form of PD-S2, starting from the N-terminal part (N-terminal sequence: 1-VSTITFDVGS ATISKYTTFL ESLRN-QAKDP-30) [24]. Furthermore, the analysis of the band at 6.5 kDa proved that it corresponded to the C-terminal portion of the protein, starting with Arg196 (N-terminal sequence of the first 30 residues: RAFYPNAKVL NLEETWGKIS MAIHGAKNGA; Fig. S2). In order to characterize cutPD-S2, we decided to purify it to homogeneity as reported in the Supplementary materials (Fig. 1A and B). The behavior of cutPD-S2 in the SDS–PAGE analysis can be rationalised taking into account the previously determined PD-S2 amino acid sequence and the S–S pairing [14,24]. The migration of cutPD-S2 as a single band in non-reducing conditions is due to the existence of a disulfide bridge between Cys34 and Cys262, which holds together the two protein ends (Fig. 1C and D, panel a). Differently, these two portions migrate as two separate bands when the disulfide bridge Cys34–Cys262 is reduced with β-mercaptoethanol in the SDS–PAGE (Fig. 1C and D, panel b).

3.2. Structural stability of cutPD-S2 to thermal and chemical treatment

CD spectroscopy was adopted to analyse the structural integrity of cutPD-S2, compared to native PD-S2 and hplcPD-S2 (see Section 2, Fig. 2A). CD spectra of all proteins were superimposable and showed the typical features of α–β proteins, with two minima at 222 and 208 nm, and a positive maximum at 190 nm. This suggests that the three proteins share the same secondary structure. We also investigated the thermal stability of cutPD-S2, compared to its uncleaved counterpart, by performing CD spectroscopy thermal denaturation studies. In all measurements, we observed that PD-S2 unfolds cooperatively (Fig. 2B). However, cutPD-S2 exhibited a significantly lower thermal stability (T_m 83 °C), compared to native PD-S2 (T_m 89 °C), whereas only marginal differences were measured between the two controls (native and hplcPD-S2, Fig. 2B). These results show that the proteolytic cleavage between Asn195 and Arg196 significantly destabilized the native PD-S2 fold.

To monitor the extent of the interactions between the N- and C-terminal portions of cutPD-S2, we performed selective reduction by using different amounts of DTT (protein:DTT ratios of 1:5 and 1:10) and quantified the amount of the released C-terminal portion

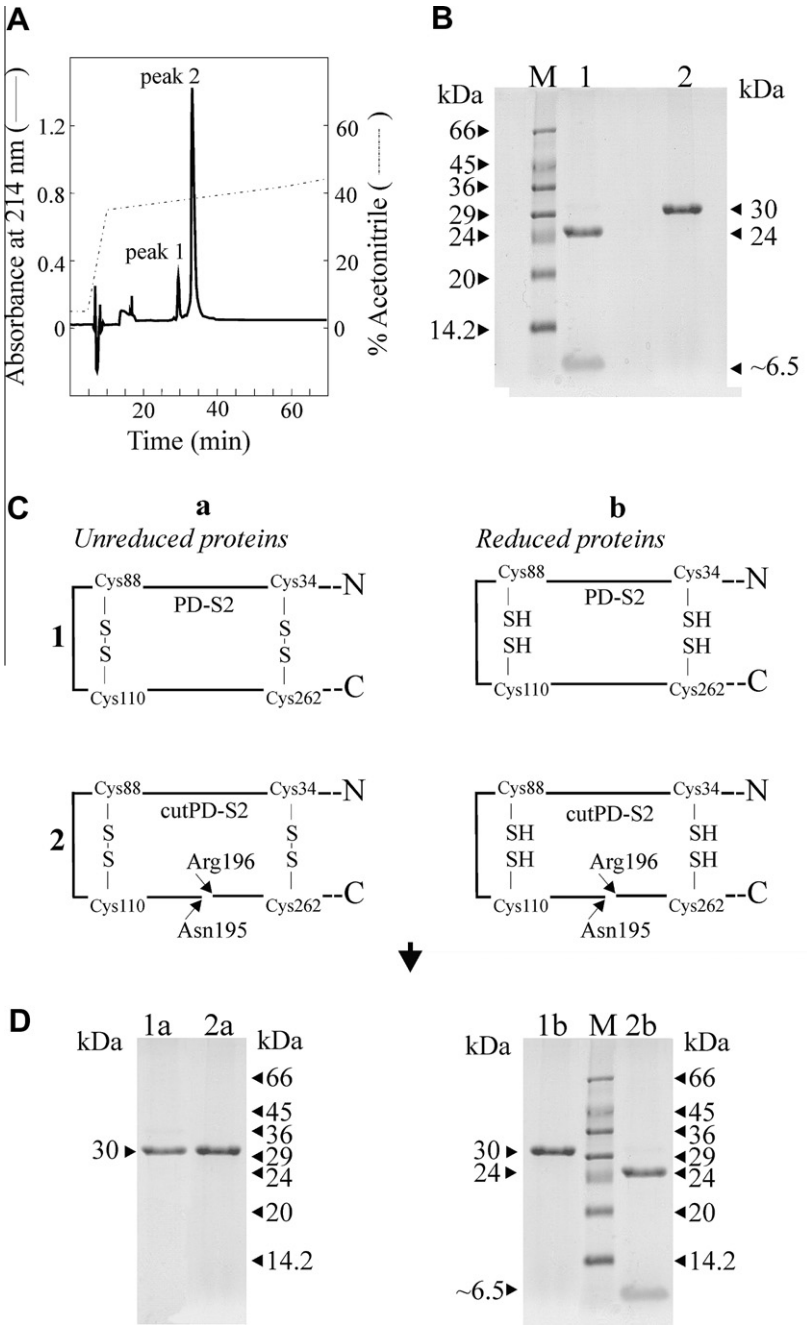

Fig. 1. (A) RP-HPLC separation of cutPD-S2 (peak 1), from the ascending part of the PD-S2 peak from the CM-Sepharose chromatography (gray color in Fig. S1). (B) SDS–PAGE analysis of peak 1 of A, with or without 2-Me (1 and 2, respectively). (C) Schematic structure of cutPD-S2 (1) and native PD-S2 (2) with and without reducing agent. (D) SDS–PAGE analysis of cutPD-S2 and native PD-S2 (lanes 1 and 2) without 2-Me and 1b and 2b with 2-Me. M, molecular weight markers.

by HPLC. Furthermore, we adopted increasing concentrations of Gdn · Cl as a denaturant agent to check the dependence of the fragment release on the protein structural integrity. Our results showed that, using a protein DTT ratio of 1:5, there was no release of the peptide in non-denaturing conditions (no Gdn · Cl). This result suggests that strong non-covalent interactions exist between the PD-S2 fold and the C-terminal peptide. By increasing the Gdn · Cl concentration, we observed a sigmoidal increase of released peptide, with a full release only at a concentration of Gdn · Cl as high as 5 M (Fig. 2C). Interestingly, this Gdn · Cl well compared with the C_m of Gdn · Cl induced chemical denaturation, measured by CD spectroscopy (Fig. 2D). Therefore, the full release of the C-terminal portion was obtained only when the protein was completely chemically denaturated (Fig. 2D). To check the different susceptibilities to reduction of the two disulfide bonds of cutPD-S2 (Fig. S2), we also alkylated samples at an intermediate level of protein reduction (Fig. 2C, Gdn · Cl concentration 4 M) and evaluated the extent of *S*-carboxymethylcysteine formation. Amino acids analyses showed that, using 4 M Gdn · Cl, only the Cys34–Cys262 bridge was reduced. Reduction of the Cys88–Cys110 disulfide bond required a higher DTT concentration (protein:DTT ratio 1:10). Therefore, these results show that the disulfide bond Cys34–Cys262, responsible for peptide release, is also the most susceptible to reduction.

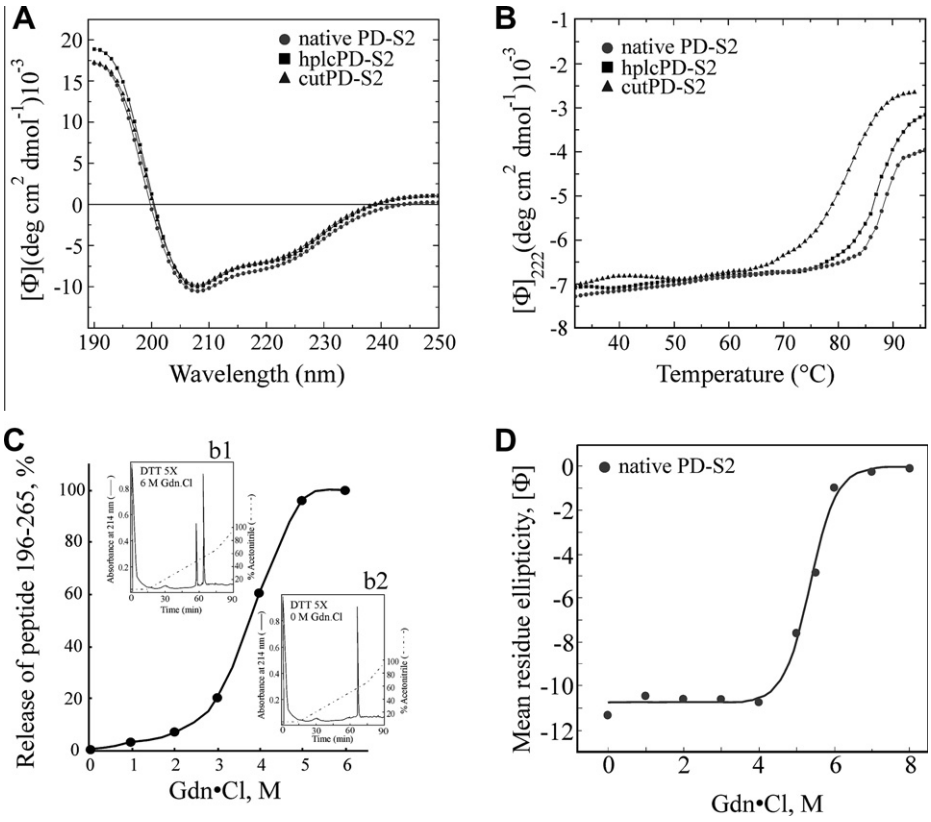

Fig. 2. (A) CD spectra of cutPD-S2 (▲), hplcPD-S2 RP (■), and native PD-S2 (●). (B) Thermal denaturation profile of cutPD-S2 (▲), hplcPD-S2 (■) and native PD-S2 (●). (C) Release of the C-terminal peptide (196–265) after selective reduction of cutPD-S2 with 5× DTT on the protein (mol:mol) and increasing Gdn · Cl concentrations (see text). In the insets b1 and b2: RP-HPLC elution profile of cutPD-S2 with DTT at 6 and 0 M Gdn · Cl, respectively. (D) Gdn · Cl-induced denaturation of native PD-S2; experimental values are fitted with a sigmoidal curve.

3.3. Ribosome inactivating activity of cutPD-S2

The effect of the proteolytic cleavage between Asn195 and Arg196 on the enzyme activity of cutPD-S2 was assayed by measuring its inhibitory activity on protein synthesis in a rabbit reticulocyte cell-free system (see Section 2), including pT7 luciferase DNA (plasmid pT7-luc). In this system, mRNA coding for luciferase is transcribed from the plasmid pT7-luc using T7 RNA polymerase. Subsequently, the active protein is synthesized by the translation system of the reticulocyte lysate and the relative amount of luciferase generated is monitored in a bioluminescence assay. The latter is based on the measurement of light emission by the excited product from the oxidization of luciferin catalyzed by luciferase. The addition of RIP leads to an inactivation of the ribosomes and therefore, the yield of active luciferase compared to the control decreases. Results obtained for cutPD-S2, in comparison with those of native and hplcPD-S2 (Fig. 3A), showed that all assayed proteins hampered protein translation, as evidenced by the decrease of luciferase activity with an increasing protein concentration. However, a strikingly different IC_{50} value characterized cutPD-S2, when compared to hplcPD-S2 and native PD-S2. Indeed, the IC_{50} value for cutPD-S2 (74.03 pM) was more than 370 times lower than those of corresponding uncleaved forms (IC_{50} of 0.2 and 0.3 pM for native and hplcPD-S2, respectively).

However, the effect of Asn195–Arg196 cleavage was barely evident when the APG activity was assayed on hsDNA and poly(A) substrates. Indeed, the observed decrease in enzyme functionality could be only partially related to proteolysis and more so to the HPLC/refolding treatment. Indeed, when hsDNA was used as substrate, activity reduction of 26.67% and 14.76%, compared to native PD-S2, were measured for cutPD-S2 and hplcPD-S2, respectively. Similarly, when poly(A) was used as a substrate, activity reduction was 40.78% and 34.69%, respectively (Fig. 4B). The effect which could be ascribed to the peptide bond cleavage between Asn195–Arg196 would be 12% and 6%, respectively.

Overall, our results clearly show that Asn195–Arg196 cleavage has a strong impact on protein synthesis by ribosomes, whereas it has barely any effect on deadenylation of hsDNA and poly(A) substrates.

3.4. Structural determinants of PD-S2 inactivation

To investigate the structural determinants responsible of the cutPD-S2 activity decrease, compared to PD-S2, we carried out homology modeling studies. Highest sequence identity, calculated by BLAST sequence analyses, was found with the pokeweed antiviral protein (78%; pdb code 1APA). Modeling of PD-S2 (Fig. 4) showed that the proteolytic cleavage present in cutPD-S2 (Fig. 1C and D) was located in the loop between helix 7 and helix 8. The 3D structure showed tight interactions between the N- and the C-terminal ends of the protein and that the catalytic site was made up by both parts. A large contact surface, of 1869 $Å^2$, characterized the interface between the N- and C-terminal regions of the protein. This well explained our results showing that a full release of the C-terminal region in cutPD-S2 was observed only upon protein chemical denaturation (Fig. 2C).

Although not in the immediate vicinity of the main catalytic residues, the Asn195–Arg196 cleavage site is located in the catalytic site cleft of the enzyme. Notably, the proteolytic cleavage between Asn195 and Arg196 adds two extra charges, as confirmed by different retention times in the HPLC profiles. Indeed, consistent with a higher hydrophilicity induced by the cleavage, cutPD-S2

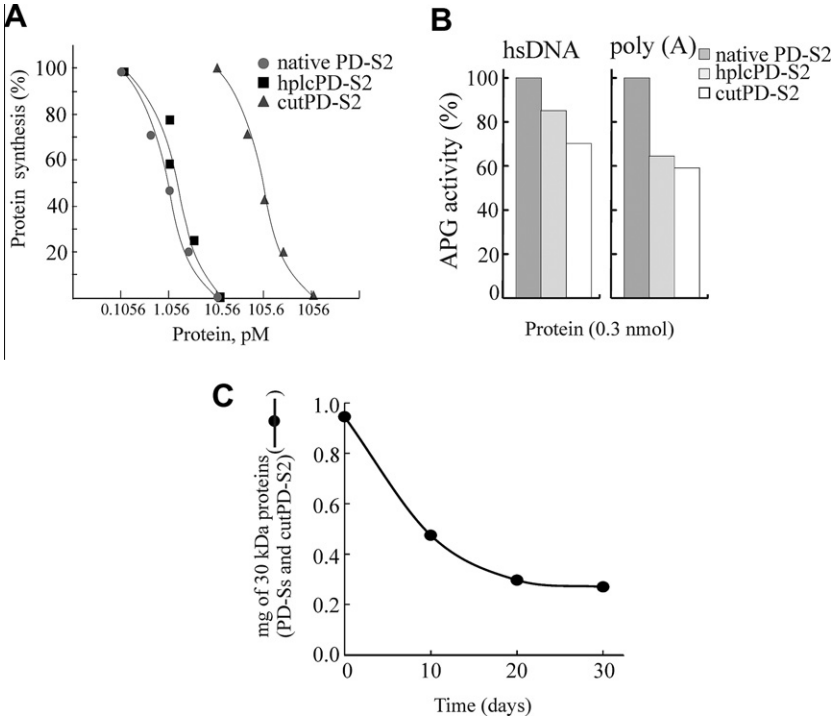

Fig. 3. (A) Inhibition of protein synthesis by cutPD-S2 (▲), hplcPD-S2 (■), and native PD-S2 (●). The graphs show protein synthesis determined measuring the luciferase activity in a lysate of rabbit reticulocytes. (B) Adenine polynucleotide glycosidase activity of native PD-S2, hplcPD-S2 and cutPD-S2 assayed on hsDNA or poly(A). Data are reported as percentage of native PD-S2 activity. (C) Milligrams of ~30 kDa basic proteins (30 kDa peak from the gel-filtration) extracted from 2 g of *P. dioica* seedlings at different days after germination (10, 20 and 30 days), referred to the proteins extracted from 2 g of seeds. Standard deviations were <5% for each experiment.

eluted at lower retention times (about 3 min), compared to PD-S2 (Fig. 1A). This observation may well explain the different results we obtained on protein biosynthesis by ribosomes, compared to the deadenylation of hsDNA and poly(A) substrates. Indeed, the presence of two extra-charges, due to the cleavage of a peptide bond, very likely alters binding of cutPD-S2 to the ribosome-sarcin loop, while it has only a moderate effect on the binding of more flexible substrates, like hsDNA and poly(A).

3.5. Fate of PD-Ss during seed germination

The total amount of PD-S1 (7 mg/100 g seeds), PD-S2 (86 mg/100 g) and PD-S3 (3.4 mg/100 g) was 96.4 mg/100 g dormant seeds. They account for 2.40% of total seed proteins. We then investigated the fate of these proteins during seed germination to form seedlings, monitoring their amount at increasing germination times. In particular, seeds were placed in a germinator at 24 °C and collected after 10, 20 and 30 days. A control experiment was performed using seeds before they were incubated in the germinator. After seed collection, the amount of PD-Ss was obtained quantifying, using the BCA assay, the proteins contained in the 30 kDa peak from the gel-filtration (Fig. S1). We observed that the amount of PD-Ss decreased with the germination time, with a complete disappearance after 30 days. At all investigated germination times, a form of PD-Ss, with a lower molecular weight, compatible with cutPD-S2 (24 kDa), was observed both using SDS–PAGE and the RP-HPLC analysis. This form was found to be only 3% of the intact form. Furthermore, Edman degradation experiments confirmed the presence of two N-terminal sequences, typical of cutPD-S2.

4. Discussion

Proteolysis mediated by asparagine-specific endopeptidases is a typical phenomenon involved in storage-protein mobilization during seed germination [15]. These endopeptidases, specific for asparaginyl residues in the P1 position [25], are often involved in pro-polypeptide processing and protein breakdown in plants [26]. Small amounts of endopeptidases are present in mature dry vetch seeds at the time of germination and during early seedling growth [27].

We observed that PD-S2, the major form of RIPs isolated from *P. dioca* mature seeds [8], contained a proteolytic form, here named cutPD-S2. Notably, cutPD-S2 exhibited a significantly lower thermal stability, compared to PD-S2 (Fig. 2B) and a 370-fold depressed activity on protein biosynthesis by ribosomes (Fig. 3A). cutPD-S2 is generated from native PD-S2 by a specific proteolytic cleavage between the amino acid residues Asn195 and Arg196. Homology modeling studies showed that the observed cleavage is in the loop connecting helix 7 and helix 8, and divides the protein into two tightly interacting portions (Fig. 4). Therefore, the catalytic site is composed of both residues of the N- (1–195) and of the C-terminal (196–265) portions of the protein (Fig. 4A). These portions in cutPD-S2 are covalently connected by a disulfide bridge between Cys34 and Cys262, which can be reduced, allowing the release of the C-terminal part of cutPD-S2 only upon chemical denaturation (Fig. 2C and D). The proteolytic cleavage between Asn195 and Arg195 adds two extra-charges, as confirmed by different retention times in the HPLC profiles (Fig. 1A). Our results identify this feature as a main structural determinant of the observed depressed activity of cutPD-S2 against ribosomes (Fig. 4D), but not against hsDNA and poly(A) (Fig. 3B). Indeed, the presence of extra-charges in the site of interaction with ribosomes likely strongly effects binding affinity of cutPD-S2 to its natural substrates, without significantly affecting binding affinity of flexible substrates, like hsDNA and poly(A).

Our results, showing that *P. dioica* seeds produce the nearly inactive cutPD-S2 even in the presence of protease inhibitors, suggest that, as observed for ricin [17], cutPD-S2 is involved in a regulative process governed by asparagine-specific endopeptidases(s) [27,28]. The specific proteolytic cleavage between Asn195 and

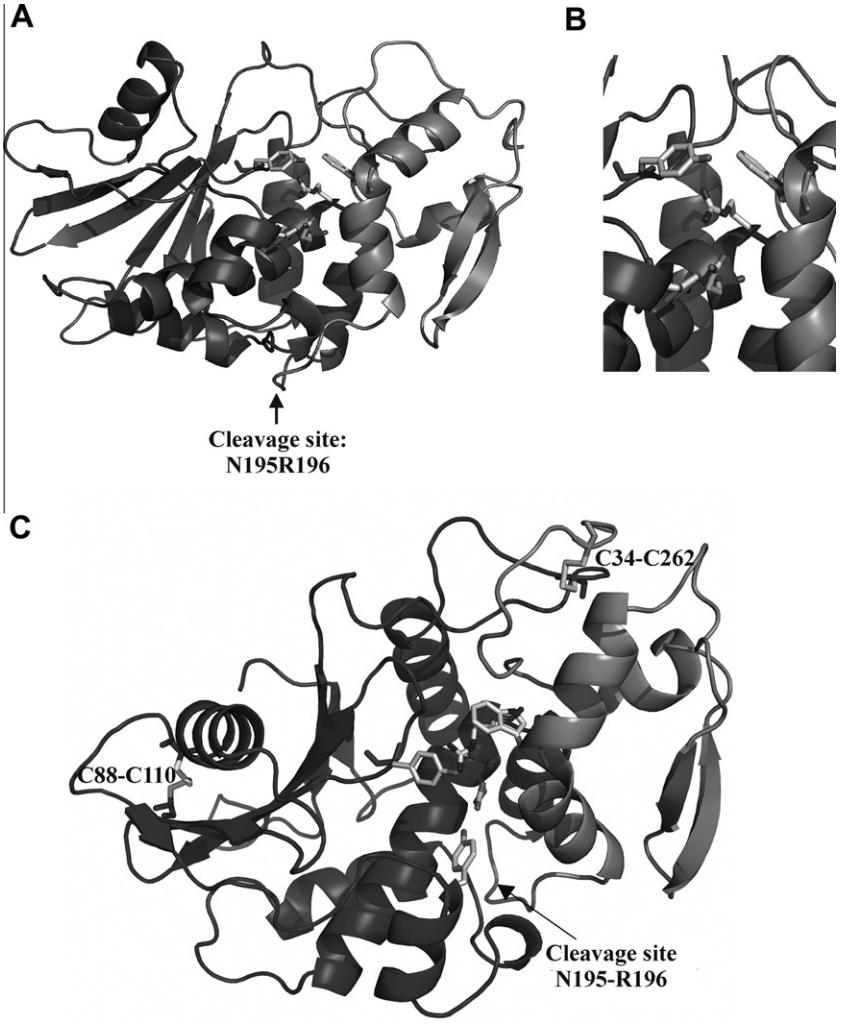

Fig. 4. 3D-structure of PD-S2 derived from molecular modeling. (A) Ribbon representation of the overall structure. The Asn195–Arg196 cleavage site is highlighted by an arrow, and the N- and C-terminal PD-S2 portions are colored purple and orange, respectively. (B) A detail of the PD-S2 catalytic site, formed by both N- and C-terminal portions. (C) Ribbon representation showing Asn195–Arg196 cleavage site along the PD-S2 binding cleft. Disulfide bonds are drawn in yellow stick representation.

Arg195 in PD-S2, may be the initial event leading to subsequent degradation of this RIP (Fig. S3). In fact, our data on the fate of PD-S2 during germination of seeds to form seedlings show that the amount of PD-S2 decreases with germination time, with a complete disappearance after 30 days, whereas the ratio between cut-PD-S2 and PD-S2 remains constant (3%). Disappearance of PD-S2 after 30 days is protective during the early stages of development, when the seedling is likely vulnerable. During this time, any stray PD-S2 molecules would likely result in a nonviable or weak seedling as reported for other RIPs [17]. These data are in agreement with our previous results that detected the presence of *P. dioica* RIPs (in particular, dioicin 1) only at the stage of young plants [12]. Overall, our results indicate that the presence of *P. dioica* RIPs is developmentally regulated, not only by gene regulation [29] but also by post-translational proteolytic processing [17].

Acknowledgment

This research was supported by grants from the Seconda Università di Napoli.

Appendix A. Supplementary data

Supplementary data associated with this article can be found, in the online version, at http://dx.doi.org/10.1016/j.bbrc.2012.04.036.

References

[1] T. Girbes, J.M. Ferreras, F.J. Arias, F. Stirpe, Description, distribution, activity and phylogenetic relationship of ribosome-inactivating proteins in plants, fungi and bacteria, Mini Rev. Med. Chem. 4 (2004) 461–476.

[2] L. Barbieri, M.G. Battelli, F. Stirpe, Ribosome-inactivating proteins from plants, Biochim. Biophys. Acta 1154 (1993) 237–282.

[3] A. Zhabokritsky, M. Kutky, L.A. Burns, R.A. Karran, K.A. Hudak, RNA toxins: mediators of stress adaptation and pathogen defense, Wiley Interdiscip. Rev. RNA 2 (2011) 900–903.

[4] M. Wang, K.A. Hudak, Applications of plant antiviral proteins, Genet. Eng. (NY) 25 (2003) 143–161.

[5] F. Stirpe, M.G. Battelli, Ribosome-inactivating proteins: progress and problems, Cell. Mol. Life Sci. 63 (2006) 1850–1866.

[6] G. Corrado, P. Delli Bovi, R. Ciliento, L. Gaudio, A. Di Maro, S. Aceto, M. Lorito, R. Rao, Inducible expression of a *Phytolacca heterotepala* ribosome-inactivating protein leads to enhanced resistance against major fungal pathogens in tobacco, Phytopathology 95 (2005) 206–215.

[7] M. de Virgilio, A. Lombardi, R. Caliandro, M.S. Fabbrini, Ribosome-inactivating proteins: from plant defense to tumor attack, Toxins 2 (2010) 2699–2737.

[8] A. Parente, R. Berisio, A. Chambery, A. Di Maro, Type 1 ribosome-inactivating proteins from the Ombú Tree (*Phytolacca dioica* L.), in: L.M. Lord, M.R.R. Hartley (Eds.), Toxic Plant Proteins, Springer-Verlag, Berlin, Heidelberg, 2010, pp. 79–106.

[9] A. Di Maro, P. Valbonesi, A. Bolognesi, F. Stirpe, P. De Luca, G. Siniscalco Gigliano, L. Gaudio, P. Delli Bovi, P. Ferranti, A. Malorni, A. Parente, Isolation and characterization of four type-1 ribosome-inactivating proteins, with polynucleotide:adenosine glycosidase activity, from leaves of *Phytolacca dioica* L., Planta 208 (1999) 125–131.

[10] A. Di Maro, A. Chambery, V. Carafa, S. Costantini, G. Colonna, A. Parente, Structural characterization and comparative modeling of PD-Ls 1–3, type 1

ribosome-inactivating proteins from summer leaves of *Phytolacca dioica* L., Biochimie 91 (2009) 352–363.

[11] S. Aceto, A. Di Maro, B. Conforto, G.G. Siniscalco, A. Parente, P. Delli Bovi, L. Gaudio, Nicking activity on pBR322 DNA of ribosome inactivating proteins from *Phytolacca dioica* L. leaves, Biol. Chem. 386 (2005) 307–317.

[12] A. Parente, B. Conforto, A. Di Maro, A. Chambery, P. De Luca, A. Bolognesi, M. Iriti, F. Faoro, Type 1 ribosome-inactivating proteins from *Phytolacca dioica* L. leaves: differential seasonal and age expression, and cellular localization, Planta 228 (2008) 963–975.

[13] A. Parente, P. De Luca, A. Bolognesi, L. Barbieri, M.G. Battelli, A. Abbondanza, M.J. Sande, G.S. Gigliano, P.L. Tazzari, F. Stirpe, Purification and partial characterization of single-chain ribosome-inactivating proteins from the seeds of *Phytolacca dioica* L., Biochim. Biophys. Acta 1216 (1993) 43–49.

[14] A. Chambery, A. Di Maro, A. Parente, Primary structure and glycan moiety characterization of PD-Ss, type 1 ribosome-inactivating proteins from *Phytolacca dioica* L. seeds, by precursor ion discovery on a Q-TOF mass spectrometer, Phytochemistry 69 (2008) 1973–1982.

[15] A.D. Shutov, I.A. Vaintraub, Degradation of storage proteins in germinating seeds, Phytochemistry 26 (1987) 1557–1566.

[16] K. Muntz, M.A. Belozersky, Y.E. Dunaevsky, A. Schlereth, J. Tiedemann, Stored proteinases and the initiation of storage protein mobilization in seeds during germination and seedling growth, J. Exp. Bot. 52 (2001) 1741–1752.

[17] D.J. Barnesa, B.S. Baldwinb, D.A. Braascha, Ricin accumulation and degradation during castor seed development and late germination, Ind. Crops Prod. 30 (2009) 254–258.

[18] U.K. Laemmli, R.A. Johnson, Maturation of the head of bacteriophage T4. II. Head-related, aberrant tau-particles, J. Mol. Biol. 80 (1973) 601–611.

[19] W.C. Johnson Jr., Analysis of circular dichroism spectra, Methods Enzymol. 210 (1992) 426–447.

[20] A. Di Maro, A. Chambery, A. Daniele, P. Casoria, A. Parente, Isolation and characterization of heterotepalins, type 1 ribosome-inactivating proteins from *Phytolacca heterotepala* leaves, Phytochemistry 68 (2007) 767–776.

[21] L. Barbieri, P. Valbonesi, E. Bonora, P. Gorini, A. Bolognesi, F. Stirpe, Polynucleotide:adenosine glycosidase activity of ribosome-inactivating proteins: effect on DNA, RNA and poly(A), Nucleic Acids Res. 25 (1997) 518–522.

[22] L. Bordoli, F. Kiefer, K. Arnold, P. Benkert, J. Battey, T. Schwede, Protein structure homology modeling using SWISS-MODEL workspace, Nat. Protoc. 4 (2009) 1–13.

[23] D. Van Der Spoel, E. Lindahl, B. Hess, G. Groenhof, A.E. Mark, H.J. Berendsen, GROMACS: fast, flexible, and free, J. Comput. Chem. 26 (2005) 1701–1718.

[24] F. Del Vecchio Blanco, A. Bolognesi, A. Malorni, M.J. Sande, G. Savino, A. Parente, Complete amino-acid sequence of PD-S2, a new ribosome-inactivating protein from seeds of *Phytolacca dioica* L., Biochim. Biophys. Acta 1338 (1997) 137–144.

[25] S. Odani, T. Ikenaka, Scission of soybean Bowman–Birk proteinase inhibitor into two small fragments having either trypsin or chymotrypsin inhibitory activity, J. Biochem. 74 (1973) 857–860.

[26] K.A. Müntz, F.R.A. Blattner, A.D.B. Shutov, Legumains – a family of asparagine-specific cysteine endopeptidases involved in propolypeptide processing and protein breakdown in plants, J. Plant Physiol. 159 (2002) 1281–1293.

[27] K. Muntz, A.D. Shutov, Legumains and their functions in plants, Trends Plant Sci. 7 (2002) 340–344.

[28] A.D. Shutov, F.R. Blattner, I.A. Kakhovskaya, K. Muntz, New aspects of the molecular evolution of legumains, Asn-specific cysteine proteinases, J. Plant Physiol. 169 (2011) 319–321.

[29] R. Iglesias, Y. Perez, L. Citores, J.M. Ferreras, E. Mendez, T. Girbes, Elicitor-dependent expression of the ribosome-inactivating protein beetin is developmentally regulated, J. Exp. Bot. 59 (2008) 1215–1223.